# Diagnostic accuracy of ultrasound and MRI in parotid gland tumors: A retrospective study

JIN KUANG[1*], QIAN RAO[2*] and ZHIGANG CHENG[1]

[1]Department of Stomatology, Central Hospital of Wuhan, Tongji Medical College, Huazhong University of Science and Technology, Wuhan, Hubei 430014, P.R. China; [2]Department of Stomatology, Wuhan Children's Hospital (Wuhan Maternal and Child Healthcare Hospital), Tongji Medical College, Huazhong University of Science and Technology, Wuhan, Hubei 430014, P.R. China

Received July 15, 2024; Accepted June 17, 2025

DOI: 10.3892/etm.2025.12920

**Abstract.** Parotid gland tumors (PGTs) are the most common salivary gland neoplasms, encompassing diverse benign and malignant pathologies. Accurate preoperative diagnosis is vital for surgical planning, functional outcomes (e.g., facial nerve preservation), and prognosis. While histopathology remains the gold standard, non-invasive imaging, such as ultrasound (US) and MRI, plays a critical role in initial tumor characterization. US is widely used due to its accessibility and cost-effectiveness, but its utility is constrained by acoustic limitations and operator dependence. MRI, with superior soft tissue contrast and multiplanar capabilities, excels in delineating tumor extent and neural involvement but often struggles to differentiate benign from malignant lesions due to overlapping imaging features. The comparisons of diagnostic performance between US and MRI limited, and optimal imaging parameters for specific PGT subtypes remain underinvestigated. The aim of the present study was to review and summarize the clinical presentations and histological types of parotid tumors, whilst also evaluating the diagnostic accuracy of US and MRI, to determine optimal US imaging parameters for pleomorphic adenomas and Warthin tumors. The medical records, including imaging examination results, type of parotidectomy and postoperative pathological findings, of 214 patients with confirmed PGTs were collected from the database of Central Hospital of Wuhan (Wuhan, China). The nature of the tumor was assessed based on imaging findings (US and MRI), with postoperative pathology (hematoxylin and eosin and immunohistochemistry) used as the gold standard. The sensitivity, specificity, accuracy, positive predictive value (PPV) and negative predictive value (NPV) for US and MRI were established. The area under the curve (AUC) was computed to compare the accuracy of US and MRI in identifying the nature of parotid gland tumors. The Youden index was calculated to evaluate the diagnostic power. Data analysis was conducted using SPSS version 29.0, where statistical significance was set at $P<0.05$ using the $\chi^2$ test. In the field of PGT diagnosis, the combination of US and MRI technologies was found to significantly enhance diagnostic precision. This integrated approach showed a statistically significant improvement over the use of US alone ($P<0.05$). Although MRI, as an independent modality, showed higher accuracy compared with that of US, the difference between MRI and US was not statistically significant. The receiver operating characteristic curve analysis indicated that the AUC for MRI in diagnosing benign and malignant parotid gland tumors was 0.899, which was significantly greater compared with that of US (0.702; $P<0.001$). The combined diagnosis using US and MRI achieved the highest specificity (94.8%), compared with US (52.6%) and MRI (71.9%) alone. For the combined US-MRI approach, the PPV, NPV and Youden index were 84.6, 95.0 and 0.68%. For US and MRI alone, the PPV, NPV and Youden index were 64.7, 94.1 and 0.34%, and 75.8, 95.0 and 0.67%, respectively. To conclude, these data suggest that the amalgamation of MRI and US can provide an efficacious means of diagnosing PGTs, thereby constituting an instrumentation for the preoperative qualitative evaluation of these tumors.

*Correspondence to:* Professor Zhigang Cheng or Dr Jin Kuang, Department of Stomatology, Central Hospital of Wuhan, Tongji Medical College, Huazhong University of Science and Technology, 26 Shengli Street, Jiang'an, Wuhan, Hubei 430014, P.R. China
E-mail: czgar068@126.com
E-mail: kuangjin@outlook.com

*Contributed equally

*Key words:* parotid gland tumor, parotidectomy, ultrasound, MRI

## Introduction

Parotid gland tumors (PGTs) are the most prevalent type of salivary gland tumors, accounting for ~80% of all cases (1). The majority of PGT cases are benign, such that even if they grow to a large size, they may not present any clinical symptoms (2). During the early stages of development, malignant tumors can grow slowly without causing any noticeable symptoms, making them difficult to distinguish from benign tumors (2). This phenomenon can lead to misdiagnosis in clinical practice. Pain or tenderness in the affected area and facial nerve paralysis are frequently used as indicators of malignancy (2).

The most common PGTs are benign, with pleomorphic adenomas (PAs) accounting for 61-81% of cases, Warthin's

tumors (WTs) accounting for 15.5-38.9%, and other entities collectively constituting merely 7% (1,3-5). PAs are typically more common in female patients compared with male counterparts (3). By contrast, WT tends to be common in male patients and individuals with a high smoking history (4). Several studies have previously shown that 75.6-82.8% PCT cases are benign and 17.2-21.2% are malignant (2,6,7), with mucoepidermoid carcinoma being the most common in the latter category (2).

Early diagnosis of PGTs is crucial, since malignant parotid tumors that have been allowed to progress to advanced T stages or present with large tumors can significantly increase the risk of advancing to high-grade cancer and nodal metastasis, resulting in poor prognosis (8). In addition, protecting the facial nerve during surgical intervention for such late-stage tumors is particularly challenging, leading to a high incidence of temporary facial weakness or even permanent facial paralysis post-parotidectomy (9).

Imaging assistance is pivotal in the evaluation of patients with parotid gland lesions, guiding the determination of both timely and personalized treatment strategies. Ultrasound (US) has emerged as one of the most beneficial and cost-effective imaging methods for the assessment of salivary gland abnormalities (10). US can aid in the differential diagnosis of benign and malignant tumors by mainly locating intra- or extraglandular lesions, which is particularly helpful for the guidance of fine needle aspiration biopsy (FNAB) (10). US has inherent limitations in parotid tumor assessment, including operator dependence, the absence of standardized imaging protocols and difficulty in evaluating deep-lobe parotid tumors. In instances where US evaluations yield inconclusive results, patients may be directed toward complementary imaging investigations, such as MRI or CT scans. MRI provides superior soft tissue contrast for evaluating PGTs, including detailed morphology, disease extension and deep space involvement; however, it is susceptible to motion artifacts and provides less precise cortical bone delineation compared with CT (11,12). The main advantages of MRI over other imaging methods include the absence of ionizing radiation and improved tissue contrast resolution, which is particularly important for detecting local tumor spread, including perineural disease (10,12).

The preoperative diagnostic procedure for PGTs is instrumental in devising surgical strategies. Although malignancies necessitate stringent therapeutic interventions, benign tumors likewise mandates caution for minimizing surgical invasion or circumvent surgery altogether. This approach aims to attenuate the risks of postoperative complications, such as facial scarring and damage to the facial nerves, underscoring its importance in the comprehensive management of these conditions (13).

The aim of the present study is to evaluate the clinical diagnostic efficacy of US and MRI in distinguishing between benign and malignant PGTs, through a comprehensive review of parotid gland tumor cases, with the intent of providing insights that can be exploited for guiding surgical decision-making.

## Materials and methods

*Data collection*. The medical records of all patients with parotid gland masses who were treated at Wuhan Central Hospital affiliated with Tongji Medical College of Huazhong University of Science and Technology (Wuhan, China) between January 2019 and December 2022 were reviewed in September 2023. Specifically, demographic information, tumor location, surgical method, pathological type and preoperative US and MRI data were obtained. The present study was approved by the ethics committee of Wuhan Central Hospital (approval no. WHZXKYL2023-117).

Inclusion criteria were as follows: i) Parotid tumors confirmed by surgical or biopsy pathology; ii) preoperative assessment, including both MRI and US; iii) tumor size >1 cm in diameter; iv) imaging clear and free from artifacts.

Exclusion criteria were as follows: i) Non-neoplastic lesions, metastatic tumors and lymphomas; ii) the absence of both MRI and US examinations, or the availability of only one imaging modality (either MRI or US alone); and iii) susceptibility artifacts (MRI) or acoustic shadowing (US) of the tumor area.

Cases of bilateral tumors with identical pathology were considered one occurrence. A tumor exhibiting both benign and malignant characteristics was categorized as malignant. In instances where multiple tumors were present, then the attributes of the largest tumor dictated the overall classification. All patients who tested positive for Coronavirus disease 2019 (COVID-19) were excluded from the present study.

*Surgical methods*. The present study applied the following three surgical approaches: Partial superficial parotidectomy (PSP); superficial parotidectomy (SP); and total parotidectomy (TPE).

SP involves identifying the facial nerve's main trunk and removing the gland's superficial portion whilst protecting its branches (14). For benign tumors, the surgical methods used are PSP and SP (14). For low-grade, early-stage tumors confined to the superficial lobe, SP may suffice, with the plane of the facial nerve branches defining the deep surgical margin (15). Compared with superficial lobectomy, partial resection of the parotid gland has a lower rate of complications, such as postoperative paralysis, salivary fistula and Frey's syndrome, due to fewer facial nerve dissections (16). For high-grade and/or high-stage tumors, or big benign tumors that involve almost all the parotid gland, a total parotidectomy is recommended (17,18). Preserving facial nerve function is critical for postoperative quality of life, mandating maximal efforts to maintain its neurophysiological integrity during resection, irrespective of tumor pathology (benign or malignant) (19). The facial nerve should be preserved if preoperatively functional and dissectible from tumor. For preoperative paresis, neurolysis should be attempted, as compression may cause reversible dysfunction. If intraoperative macroscopic invasion is confirmed, the invaded facial nerve segment should be sacrificed and immediately reconstruct via interpositional grafts/anastomosis (20,21).

*Examination methods and evaluation criteria*. MRI was conducted using the Siemens 3.0T MAGNETOM Skyra (Siemens Healthineers) with a standard head coil. T1-weighted image and T2-weighted image (T2WI) sequences, as well as short $\tau$ inversion recovery sequences, were obtained, achieving a minimal lesion resolution of 3 mm in both axial and coronal

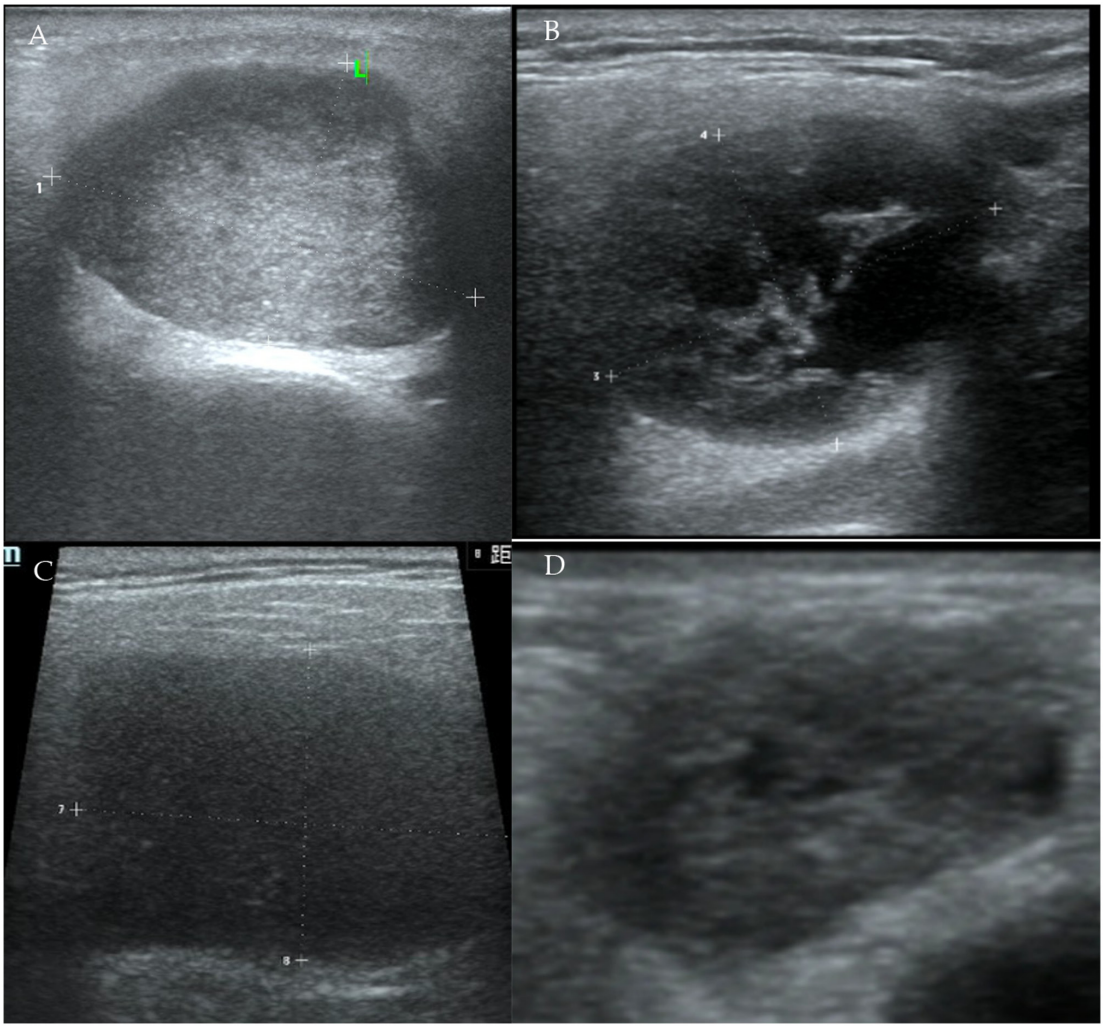


Figure 1. Echogenicity and heterogeneity of parotid gland tumors under ultrasound. (A) Slightly hypoechogenic and slightly heterogenic pleomorphic adenoma. (B) Highly hypoechogenic and highly heterogenic WT. (C) Highly hypoechogenic and slightly heterogenic WT (D) Slightly hypoechogenic and highly heterogenic mucoepidermoid carcinoma. WT, Warthin's tumor.

planes. MRI was used to reveal the dimensions of the tumor, its morphology and its relationship with deep surrounding structures. In MR images, irregular margins, extranodular extension and associated lymphadenopathy, along with low T2-weighted signal intensity and heterogeneity, may indicate malignancy (12,22). Benign tumors typically exhibit relatively uniform signal intensity, but hemorrhage and calcification can lead to a heterogeneous appearance similar to that of malignant tumors (12,23).

By contrast, US examination was performed by an US technologist with >5 years of experience in ultrasonography of the head and neck regions with Mindray DC-80 (Mindray Medical International Co., Ltd.). US assessment showed a series of characteristics, such as the tumor's size, shape (regular or irregular), homogeneity (mildly or highly heterogeneous), echogenicity (slightly hypoechoic or highly hypoechoic) and vascular pattern within the tumor (avascular or reduced vascularity, moderately vascularized or highly vascularized) (Fig. 1). A regular shape, well-defined margins, homogeneous echogenicity, a weak vascular pattern and the absence of enlarged intraparotid or cervical region lymph nodes were considered predictors of a benign tumor. However, an irregular shape, poorly defined margins and heterogeneous echogenicity were considered predictors of a malignant tumor (Fig. 2) (10,24).

The clinical and radiographic evaluations were conducted by two maxillofacial surgeons who were not involved in the patients' clinical care. These surgeons were provided with clear criteria for assessment, which were explained through five initial cases complete with a calibration exercise. The consistency between the two surgeons' success rates was measured using κ-statistics, resulting in a κ-value of 0.81, indicating a high level of agreement. On the basis of the imaging findings from US or MRI examinations, the nature of the tumor was individually assessed to determine whether it was benign or malignant (Fig. 3-5). The combined diagnosis was considered positive if either the US or MRI examination yielded a positive result. Postoperative pathology (H&E and IHC staining) served as the 'gold standard' for the present study. Tissue specimens were fixed in 10% neutral buffered formalin, embedded in paraffin and sectioned at a 4-$\mu$m thickness. Consecutive sections were stained with H&E using standard protocols (hematoxylin for 5 min and eosin for 3 min, at 25˚C) for primary histopathological assessment under a light microscope. For diagnostically

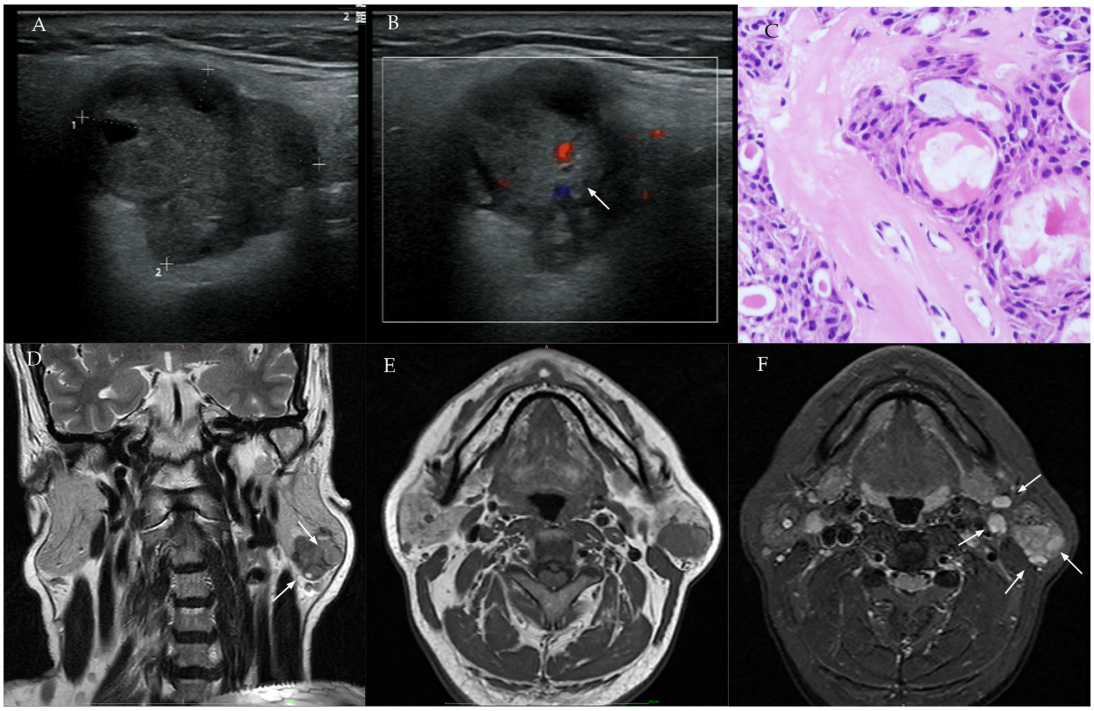


Figure 2. Features of malignant tumor (mucoepidermoid carcinoma) on US, MRI and histopathology. (A) US shows an irregularly contoured mass with indistinct margins, marked hypoechogenicity and pronounced heterogeneity. (B) Color Doppler demonstrates moderate intralesional vascularity (arrow). (C) Histopathology (H&E stain): Tumor stroma with dense lymphoid infiltration, multiple cystic formations and variably distributed epithelial nests showing squamous differentiation, intermediate cells and goblet cell metaplasia. (D) Coronal T2-weighted MRI: Irregular peripheral margins with heterogeneous signal intensity and nodular components (arrows). (E) Axial T1-weighted MRI: Homogeneous hypointensity (relative to parotid gland parenchyma). (F) Short Tau Inversion Recovery sequence: Diffuse signal heterogeneity with enlarged cervical lymph nodes (arrows). US, ultrasound.

challenging cases, IHC was utilized using standard diagnostic antibody panels performed following institutional pathology laboratory protocols to resolve classification uncertainties. The diagnostic success rates of US and MRI in identifying tumors were then compared.

*Statistical analysis*. Data were extracted from electronic medical records, encompassing: i) Demographic characteristics (age and sex); ii) clinical and social histories (disease duration and smoking status); iii) standardized imaging reports (ultrasonography and MRI); iv) surgical techniques (incision types); and v) histopathological assessments of resected specimens. Diagnostic accuracy metrics, including sensitivity, specificity, PPV and NPV were calculated based on contingency tables using the following formulae: Sensitivity=TP/(TP + FN); specificity=TN/(TN + FP); PPV=TP/(TP + FP); and NPV=TN/(TN + FN), where TP represents true positives (malignant tumors correctly classified by imaging), TN represents true negatives (benign tumors correctly classified), FP represents false positives (benign tumors misclassified as malignant) and FN represents false negatives (malignant tumors misclassified as benign).

The Youden index was also computed to evaluate diagnostic power. ROC curves were constructed to determine the predictive values, where the AUC was computed to compare the accuracy. DeLong's test was used for comparing the AUC values from the ROC curves. Data management and analysis were conducted using SPSS version 29.0 (IBM Corp.). $P<0.05$ was considered to indicate a statistically significant difference according to $\chi^2$ test.

## Results

*Baseline data*. A total of 234 PGTs were collected, where 20 cases were excluded because of incomplete data or positive COVID-19 test results. Among the remaining 214 patients (mean age, 57.92±12.75 years), 156 were male patients (72.90%; mean age, 59.04±12.29 years) and 58 were female patients (21.70%; mean age, 54.90±13.55 years). This resulted in a male-to-female ratio of 2.69:1. In addition, 97 cases (45.33%) were located on the right side, 102 cases (47.66%) were on the left side and 15 cases (7.01%) were bilateral Across the entire cohort (benign and malignant tumors), the mean disease duration was 26.76±50.22 months. The highest disease incidence occurred in patients aged 51-70 years (62.15% of all cases), with the peak incidence specifically within the 51-60 years subgroup (32.24% of total cases). In particular, there was a markedly increased incidence rate in male patients aged 51-70 years and in female patients aged 51-60 years (Table I). Amongst the cases, 192 (89.72%) involved benign tumors (mean age, 58.21±12.49 years; symptoms duration, 25.68±44.30 months), whereas 22 (10.28%) involved malignant tumors (mean age, 55.36±14.88 years; symptoms duration, 34.61±82.59 months), resulting in a benign: malignancy ratio of 8.7:1 (Table I). The male: female ratio for benign tumors is 2.84:1, whilst the same ratio for malignant tumors is 1.75:1. Furthermore, amongst the benign tumors, WT, PA and cysts accounted for the top three most common tumor types observed. By contrast, among the malignant tumors, mucoepidermoid carcinoma ranked first in terms of the number of cases observed, followed by

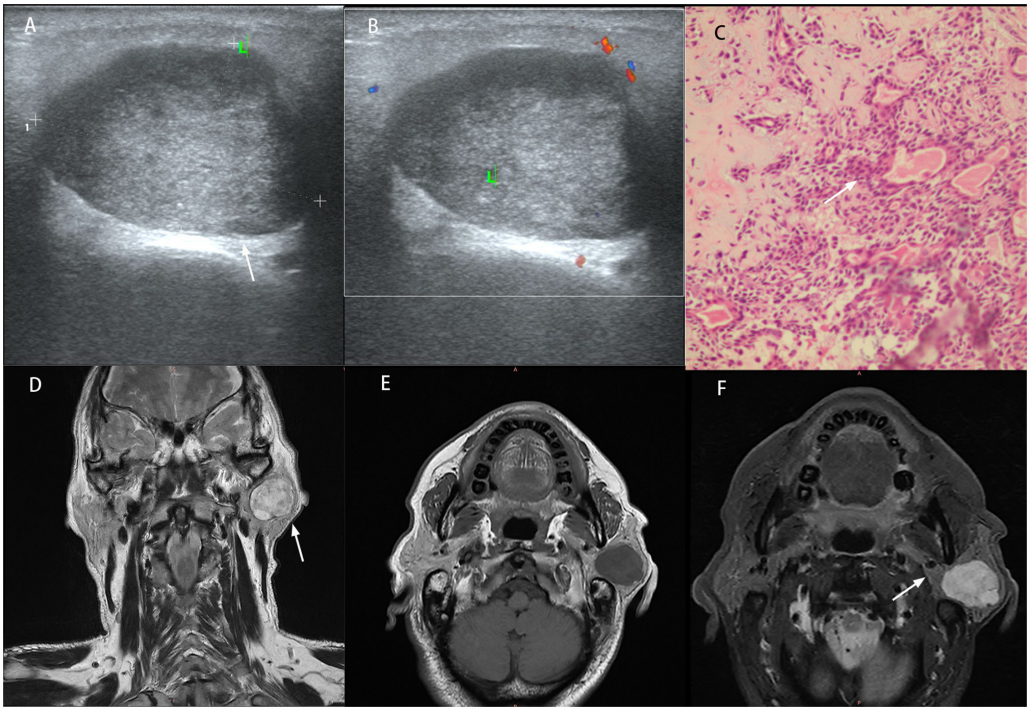


Figure 3. Features of pleomorphic adenoma on US, MRI and histopathology. (A) US: Regular contours, well-circumscribed margins (arrow) and mild hypoechogenicity. (B) Color Doppler: Homogeneous architecture without detectable vascularity. (C) Histopathology (H&E stain): Confluent sheets of epithelial/myoepithelial cells embedded in chondromyxoid stroma (arrow). (D) Coronal T2-weighted MRI: Well-defined margins (arrow) with dominant hyperintensity admixed with hypointense foci. (E) Axial T1-weighted MRI: Heterogeneous hypointensity. (F) Short Tau Inversion Recovery sequence: No abnormal lymph nodes (arrow). US, ultrasound.

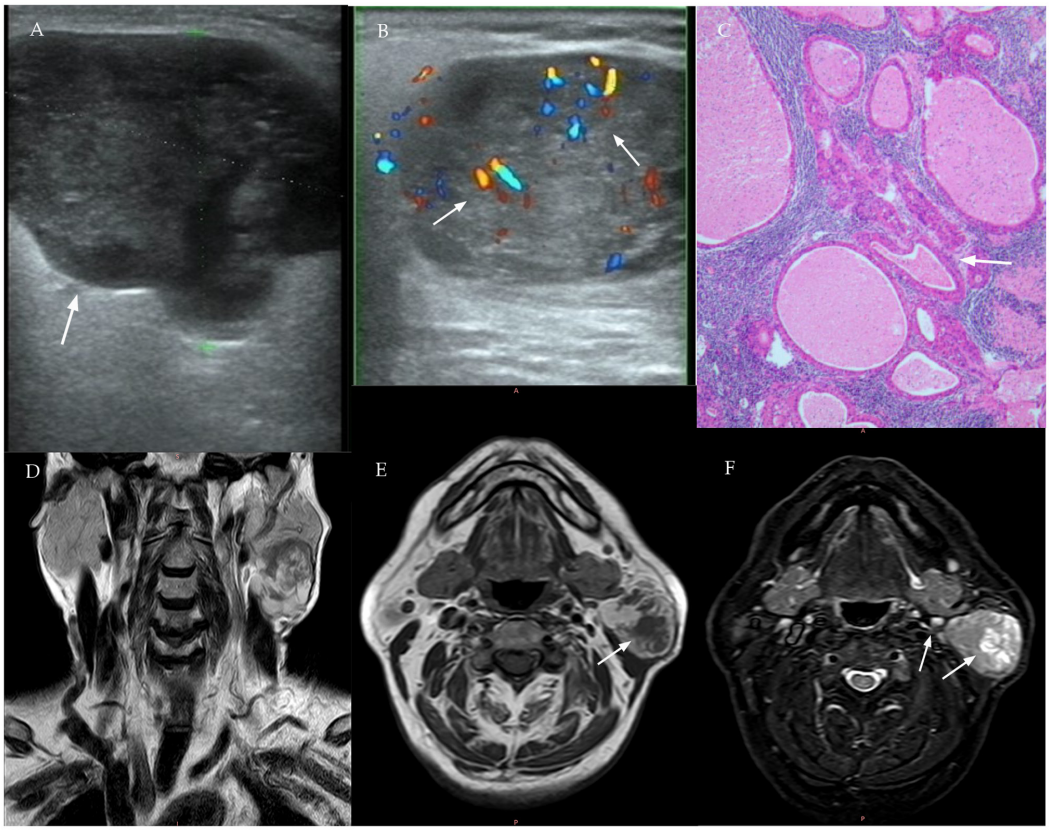


Figure 4. Features of Warthin's tumor on US, MRI and histopathology. (A) US: Irregular shape, well-defined margins (arrow), marked hypoechogenicity and mild heterogeneity. (B) Color Doppler: Intense intratumoral vascularity (arrows). (C) Histopathology (H&E stain): Bilayered oncocytic epithelium forming compact tubules within lymphoplasmacytic stroma (arrow). (D) T2-weighted MRI: Balanced proportion of hyperintense and hypointense signals. (E) T1-weighted MRI: Heterogeneous hypointensity with prominent cystic components (arrow). (F) Short Tau Inversion Recovery sequence: Intralesional cystic changes (arrow); cervical lymph nodes within normal limits (arrow). US, ultrasound.

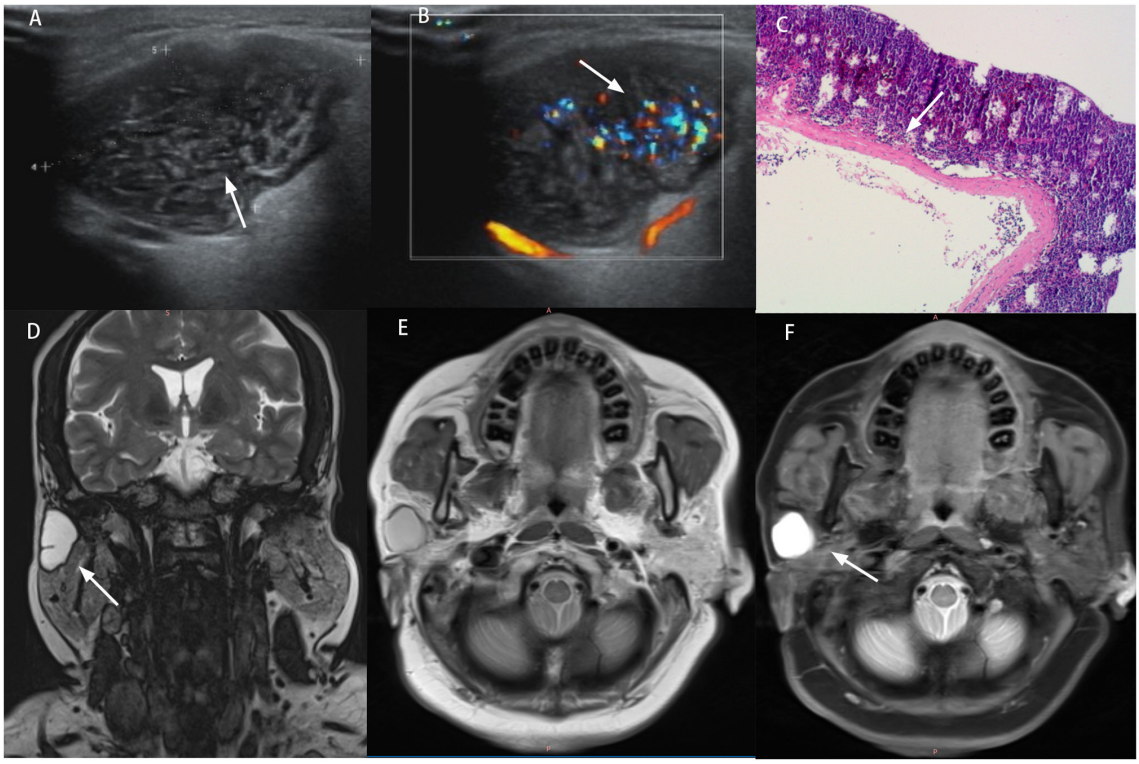


Figure 5. Features of a cyst on US, MRI and histopathology. (A) US: Irregular shape, well-defined margins, marked hypoechogenicity and moderate heterogeneity (arrow). (B) Color Doppler: Prominent intralesional vascularity (arrow). (C) Histopathology (H&E stain): Keratinizing stratified squamous epithelial lining with luminal necrotic debris (arrow). (D) T2-weighted MRI: Well-circumscribed cystic lesion with homogeneous hyperintensity (arrow). (E) T1-weighted MRI: Entirely homogeneous hyperintensity (no hypointense foci). (F) Short Tau Inversion Recovery sequence: No solid enhancement (arrow) or enlarged lymph nodes. US, ultrasound.

secretory carcinoma, adenocarcinoma and acinar cell carcinoma (Table II). In total, ~80% of the tumors were located in the superficial lobe of the parotid gland, where no significant difference was detected in the proportions of benign and malignant tumors among different sexes and anatomical sites (Table III). Table IV compares diagnostic performance of the various techniques for malignant tumors. US detected 10/22 cases (45.5%), whilst MRI identified 15/22 (68.2%). The combined MRI + US approach achieved the highest positivity rate at 18/22 (81.8%), demonstrating enhanced sensitivity. MRI alone outperformed US alone, whereas their combination yielded markedly improved diagnostic accuracy, reducing the cases of false negatives from 12 to 4. This suggests MRI's superiority and the value of multi-modality imaging for tumor detection. When comparing PAs with WTs, WT exhibited a significantly stronger association with smoking (57.0 vs. 18.1%; P<0.001). By contrast, smoking prevalence did not differ significantly between benign (38.0%) and malignant tumors (36.4%) (P=0.879) (Table V). The proportions of surgical approaches for benign tumors of the parotid gland were as follows: 38% for PSP, 43.8% for SP and 18.2% for TPE. Moreover, for malignant tumors, the proportions were 13.6, 9.1 and 72.7% for PSP, SP and TPE, respectively.

*ROC results*. Fig. 6 shows that the AUCs were 0.702 (95% CI, 0.595-0.810), 0.899 (95% CI, 0.845-0.953) and 0.841 (95% CI: 0.743-0.938) for US, MRI and US + MRI, respectively. This finding revealed a statistically significant difference in the AUC between US and MRI, in addition to between US + MRI and US. The DeLong test was used to compare AUC differences, as indicated by the reported P-values (P<0.001 and P<0.05, respectively). The sensitivity and specificity of US in differentiating malignant from benign tumors were 81.8 and 52.6%, respectively. The predictive values were calculated as follows: the PPV was 64.7% and the NPV was 94.1%. The Youden index was 0.34. For MRI, the sensitivity and specificity were 95.5 and 71.9%, respectively. The predictive values were calculated as follows: the PPV was 75.8%, and the NPV was 95%. The Youden index was 0.67. For US + MRI, the sensitivity, specificity, PPV, and NPV were 72.7, 94.8, 84.6 and 95%, respectively.

Fig. 7 shows that for hypoechogenicity and homogeneity, the AUC values were 0.694 (95% CI, 0.612-0.755) and 0.619 (95% CI, 0.554-0.685) for WT and PA, respectively. This finding suggest that hypoechogenicity and homogeneity were the most reliable parameters for differentiating between WT and PA using US (P<0.05).

## Discussion

PGTs are the most common type of salivary gland tumor, accounting for 3-8% of head and neck tumors, 75-85% of salivary gland tumors, of which the vast majority are benign (1,5). Among benign parotid tumors, PAs have the highest incidence (40-70%), followed by WTs (~30%) (25,26) and can occur at any age (27). The statistics of 214 cases of PGTs reported in the present study revealed that there were 156 male and 58 female patients, with a male-to-female ratio of 2.69:1. An

Table I. Distribution of 214 patients with parotid gland tumors [n (%)].

| | Sex | | Initial location | | | Tumor type | |
|---|---|---|---|---|---|---|---|
| Age, years | Female | Male | Left | Right | Bilateral | Benign | Malignant |
| <20 | - | 1 (0.47) | - | 1 (0.47) | - | 1 (0.47) | - |
| 21-30 | 3 (1.40) | 4 (1.87) | 4 (1.87) | 3 (1.40) | - | 5 (2.34) | 2 (0.93) |
| 31-40 | 7 (3.27) | 12 (5.61) | 9 (4.21) | 10 (4.67) | - | 16 (7.48) | 3 (1.40) |
| 41-50 | 9 (4.21) | 11 (5.14) | 12 (5.61) | 8 (3.74) | - | 20 (9.35) | - |
| 51-60 | 22 (10.28) | 47 (21.96) | 33 (15.42) | 29 (13.55) | 7 (3.27) | 61 (28.50) | 8 (3.74) |
| 61-70 | 9 (4.21) | 55 (25.70) | 28 (13.08) | 30 (14.02) | 6 (2.80) | 58 (27.10) | 6 (2.80) |
| >70 | 8 (3.74) | 26 (12.15) | 16 (7.48) | 16 (7.48) | 2 (0.93) | 31 (14.49) | 3 (1.40) |
| Total | 58 (27.10) | 156 (72.90) | 102 (47.66) | 97 (45.33) | 15 (7.01) | 192 (89.72) | 22 (10.28) |

Table II. Histopathological types of benign and malignant parotid tumors.

| Histopathology | n (%) |
|---|---|
| Benign tumors | |
| WT | 93 (48.44) |
| PA | 72 (37.50) |
| Cyst | 10 (5.21) |
| Basal cell adenoma | 7 (3.65) |
| Nodular oncocytic hyperplasia | 4 (2.08) |
| Hemangioma | 2 (1.04) |
| Lymphoepithelial sialadenitis | 2 (1.04) |
| Myoepithelioma | 1 (0.52) |
| Neurofibromas | 1 (0.52) |
| Total | 192 (100.00) |
| Malignant tumors | |
| Mucoepidermoid carcinoma | 7 (31.82) |
| Secretory carcinoma | 3 (13.64) |
| Adenocarcinoma, not otherwise specified | 3 (13.64) |
| Acinar cell carcinoma | 3 (13.64) |
| Squamous cell carcinoma | 2 (9.09) |
| Lymphoma (MALT lymphoma) | 1 (4.55) |
| Lymphoepithelial carcinoma | 1 (4.55) |
| Undifferentiated sarcoma | 1 (4.55) |
| Adenoid cystic carcinoma | 1 (4.55) |
| Total | 22 (100.00) |

WT, Warthin's tumor; PA, pleomorphic adenoma.

Table III. Analysis of parotid gland tumor characteristics [n (%)].

| Parameter | Benign tumor | Malignant tumor | $\chi^2$ | P-value |
|---|---|---|---|---|
| Location | | | 1.865 | 0.394 |
| Left | 91 (51.4) | 11 (50.0) | | |
| Right | 86 (48.6) | 11 (50.0) | | |
| Bilateral | 15 (7.8) | 0 (0.0) | | |
| Sex | | | 1.064 | 0.302 |
| Female | 50 (26.0) | 8 (36.4) | | |
| Male | 142 (74.0) | 14 (63.6) | | |

Table IV. US and MRI comparison for the diagnosis rate of malignant tumors.

| Variable | Positive, n | Negative, n | Total, n | Positive rate, % |
|---|---|---|---|---|
| US | 10 | 12 | 22 | 45.5 |
| MRI | 15 | 7 | 22 | 68.2 |
| MRI + US | 18 | 4 | 22 | 81.8 |

US, ultrasound.

age range of 51-70 years accounted for the highest incidence stage of the disease, with a composition ratio of 62.15%. Among those, an age range of 51-60 years represented peak incidence, accounting for 32.24%, where the incidence increased significantly among both male and female individuals. In the present study, patients with benign tumors were older compared with those with malignant tumors, with mean ages of 58.21±12.49 and 55.36±14.88 years, respectively. This finding contrasts with previous studies that suggested benign tumors are more common in younger age groups compared with malignant tumors (7,28). This discrepancy may be attributed to the limited number of malignant tumor cases included in the present study. In addition, amongst patients with benign tumors, male patients were more commonly affected compared with female patients, with a male:female ratio of 2.84:1. This ratio is higher but consistent with previous studies (29,30), possibly due to the predominance of WT, which accounted for 48.44% (93/192) of all cases, with male patients representing 87/93 cases. However, studies by Maahs *et al* (7) and Takahama *et al* (28) showed a female preponderance.

In the present study, there were 192 cases (89.72%) of benign tumors of the parotid gland, with the top three types

Table V. Association between smoking and different groups.

| Group | Smoking, n (%) | Not smoking, n (%) | $\chi^2$ | P-value |
|---|---|---|---|---|
| Benign subtype | | | | |
| Pleomorphic adenoma | 13 (18.1) | 59 (81.9) | 25.631 | <0.001 |
| Warthin's tumor | 53 (57.0) | 40 (43.0) | | |
| Tumor type | | | | |
| Benign | 73 (38.0) | 119 (62.0) | 0.023 | 0.879 |
| Malignant | 8 (36.4) | 14 (63.6) | | |

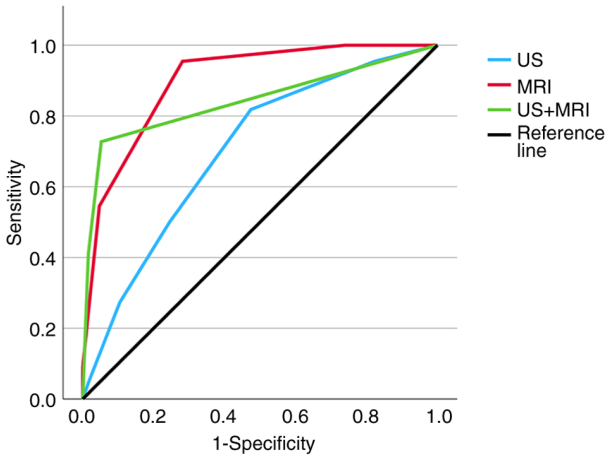


Figure 6. Receiver operating characteristics curve for US and MRI. AUC are 0.702 (95% CI, 0.595-0.810), 0.899 (95% CI, 0.845-0.953) and 0.841 (95% CI, 0.743-0.938) for US, MRI and US + MRI, respectively. The sensitivity and specificity of US in differentiating malignant from benign tumors were 81.8 and 52.6%, respectively. The predictive values were calculated as follows: PPV was 64.7% and negative NPV was 94.1%. The Youden Index was 0.34. For MRI, the sensitivity and specificity were 95.5 and 71.9%, respectively. The predictive values were calculated as follows: PPV was 75.8% and NPV was 95%. The Youden Index was 0.67. For US + MRI, the sensitivity, specificity, PPV and NPV were 72.7, 94.8, 84.6 and 95%, respectively. This indicates a statistically significant difference in accuracy between US and MRI, in addition to between US + MRI and US. AUC, area under the curve, US, ultrasound; NPV, negative predictive value; PPV, positive predictive value.

being PA, WTs and cysts. There were 22 cases (10.28%) of malignant tumors, primarily consisting of mucoepidermoid carcinoma, secretory carcinoma, adenocarcinoma and acinar cell carcinoma. The COVID-19 pandemic significantly affected patient diagnosis and surgical management, where patients delayed seeking medical care due to fears of contracting COVID-19, leading to late diagnoses. Additionally, numerous elective surgeries were postponed or canceled to free up resources for patients with COVID-19. Consequently, 20 cases were excluded due to incomplete data or positive COVID-19 test results.

Tumor location, size and histological type are the three concerns for this disease before surgery (13). Benign tumors of the parotid gland are located mostly in the superficial lobe (10,16). Before surgery, the surgical approach can be determined on the basis of the size of the tumor and imaging characteristics. It is crucial for surgeons to also seriously consider patients' clinical symptoms. Compared with benign tumors, malignant tumors tend to present more symptoms and signs, with the severity of these symptoms increasing as the grade of malignancy increases. In the cases of malignancy, facial nerve palsy and pain/tenderness are more frequently observed (2). Patients with these symptoms and signs have a significantly poorer prognosis (2,20). Pain is typically associated with the degree of malignancy instead of the size of the tumor mass (2). Benign tumors of the parotid gland can transform into malignant tumors, where it is considered that only PA can undergo malignant transformation, especially when they recur (25). According to two previous large population-based studies (25,31), the malignant conversion rate for PA recurrence was 3.2-3.3%, which was lower compared with that reported by Gunn and Parrott (23.8%) (32).

Given that surgical treatment is fundamental for parotid tumors, the choice of technique depends on the tumor's location and properties (13). Therefore, accurately distinguishing between benign and malignant tumors before surgery is crucial. Examinations of PGTs mainly include US, CT and MRI (12). US examination is convenient, time-efficient and suitable for a wide demographic of patients (33). Current US techniques have contributed to the differential diagnosis of tumors originating from the superficial lobe of the parotid gland,, as 80-90% of cases of parotid gland tumors are located in the superficial lobe (10,16,33). In general, US is the preferred diagnostic method for parotid tumors, because of its various advantages (such as low cost, easy access, non-invasive and non-radiation technology) (24,34).

US is highly precise in distinguishing tumors from other glandular abnormalities, including cysts, infections and inflammation (24). It can accurately differentiate between benign and malignant tumors, determine whether the tumor is intra- or extraglandular and offer valuable guidance for FNAB (33). Zajkowski *et al* (35) previously reported that the hypoechoic areas are more specific for WT compared with those for PA. In the present study, hypoechogenicity and homogeneity were found to be the most reliable parameters for US differentiation between the WT and PA. High-frequency US is almost as accurate as CT and MRI for diagnosing superficial lobe tumors (24,36). However, this technique is not without limitations, including operator dependence, a lack of standardized sections, low specificity for determining the histological type of parotid tumor and challenges in evaluating tumors located behind deep parotid lobes or posterior to bone structures (33,37,38).

CT is a widely accessible volumetric imaging technique that offers a soft tissue resolution but is less sensitive compared with

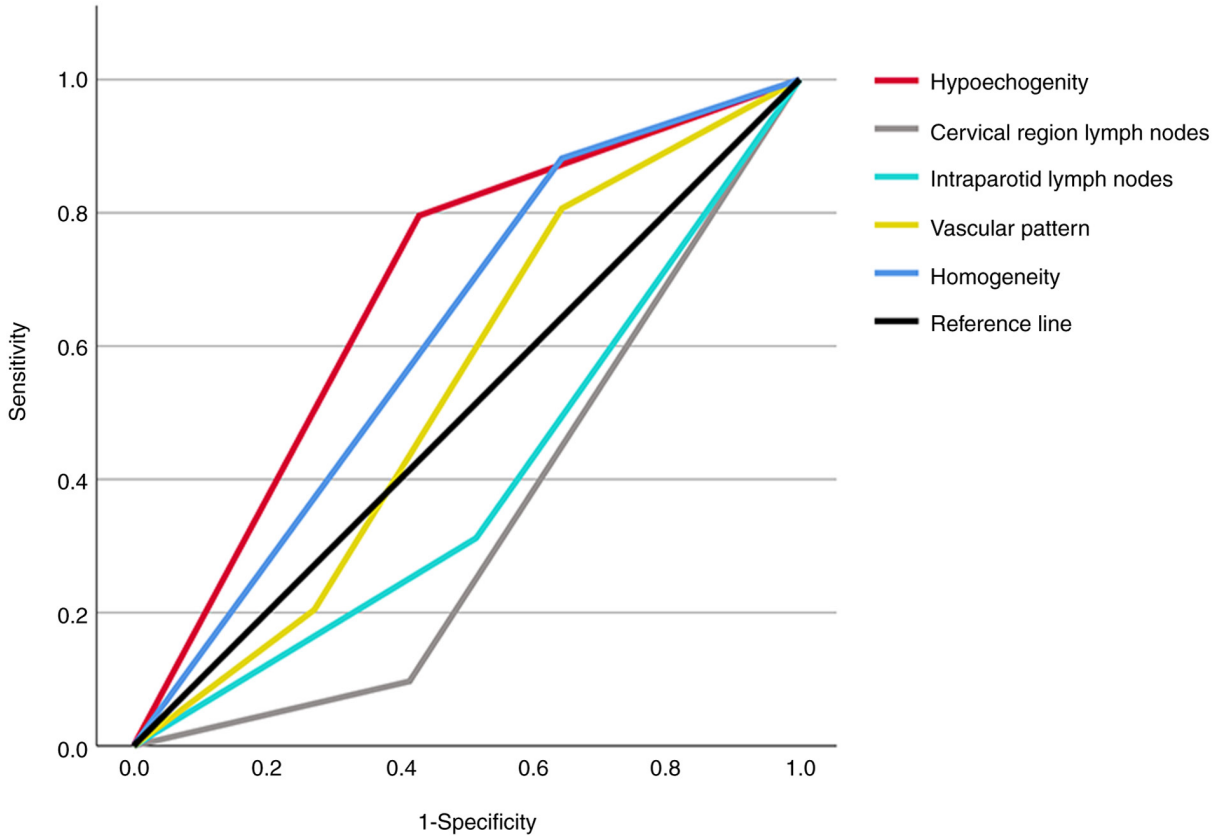


Figure 7. Receiver operating characteristic curves for WT and PA. Diagnostic performance metrics for differentiating WT from PA were as follows. Hypoechogenicity: AUC=0.694 (95% CI, 0.612-0.755); sensitivity, 79.6%; specificity, 88.2%; PPV, 67.8%; NPV, 71.2%. Homogeneity: AUC=0.619 (95% CI, 0.554-0.685); sensitivity, 57.1%; specificity, 35.7%; PPV, 69.4%; NPV, 64.6%. Hypoechogenity and homogeneity are the most reliable parameters for differentiating between WT and PA using ultrasound (P<0.05). AUC, area under the curve; PPV, positive predictive value; NPV, negative predictive value; WT, Warthin's tumors; PA, pleomorphic adenoma.

MRI (12,39). However, it does confer advantages in identifying cortical bone invasion and intratumoral calcification for the assessment of PGTs (12). Xu *et al* (40) previously established a machine learning predictive model based on CT radiomics to increase the accuracy in differentiating among PA, WT and parotid carcinoma, achieving a total accuracy of 80.5%. By contrast, MRI provides high soft tissue resolution and can identify changes in the degree of mucus production, fibrosis, cartilage matrix and hemorrhage within tumors (23). US and MRI can differentiate tumor types to some extent. PA typically appears as polycyclic or lobular shapes, with slight heterogeneity and poor vascularity, on US. By contrast, WT shows a regular shape, high heterogeneity, enlarged intraparotid lymph nodes and moderate to high vascularization (34). Previous studies also suggest that MRI-based radiomic features, Irregular margins, extraglandular extension into adjacent structures, perineural invasion and regional lymph node metastasis can distinguish between benign and malignant PGTs (41,42). Inspired by previous methodology, the present study leverages these malignancy-associated characteristics to differentiate between benign and malignant parotid gland tumors. In the present study, the diagnostic accuracy of MRI was greater compared with that of US. The accuracies for benign and malignant diagnoses by MRI were 98 and 68%, respectively. Although all the information obtained from MRI (such as lesion morphology, signal intensity and enhancement patterns) can be combined to characterize the mass, there may be overlap among the different types of tumor lesions (22). T2-weighted hypointensity and heterogeneity may suggest malignancy but are not sufficient for differentiation between benign and malignant tumors. Although benign masses frequently exhibit uniform signal intensity, hemorrhagic necrosis and calcification can also mimic malignant appearances (12,23). Previous studies have indicated that apparent diffusion coefficient measurements from diffusion-weighted imaging (DWI) have significant potential in distinguishing between benign and malignant tumors (43). However, several limitations are associated with using DWI, mainly because the sequence is acquired using the echoplanar imaging (EPI) method, which provides limited image quality, low spatial resolution and a low signal-to-noise ratio. Additionally, it is overly sensitive to blurring and artifacts (44,45). US and MRI are widely used in clinical practice because of their non-invasive nature, ease of access and lack of ionizing radiation. In the present study, the combined use of US and MRI for diagnosing malignant parotid tumors achieved an accuracy of 82%, which was greater compared with that of either modality alone, demonstrating its effectiveness. The combined diagnostic approach using US and MRI for PGTs offers significant advantages. These include complementary strengths, enhanced diagnostic accuracy, reduced risk of misdiagnosis, optimized treatment plans and advancements in medical imaging technology. This method provides clinicians with comprehensive diagnostic

information, facilitating precise treatment plans and improving patient outcomes and survival rates. Previous studies tended to rely on a single diagnostic method, but the present study applied both US and MRI to leverage their individual strengths, thereby improving accuracy whilst minimizing risks. However, potential disadvantages of the combined diagnostic approach, such as increased costs and longer examination times, must be carefully considered, with a comprehensive assessment of their impact on patient care and outcomes.

Despite these advantages, it is important to acknowledge the limitations of the present study. Operator dependence remains a significant issue, since the accuracy of both US and MRI can be influenced by the skill and experience of the radiologist. There was also a lack of standardized sections for evaluating tumors located behind deep parotid lobes or posterior to bone structures, which can complicate accurate diagnosis. Additionally, whilst CT offers valuable information about cortical bone invasion and intratumoral calcification, its soft tissue resolution is less sensitive compared with that of MRI (12,39). The reliance on DWI for distinguishing between benign and malignant tumors comes with limitations due to its acquisition using the EPI method, resulting in limited image quality, low spatial resolution and a low signal-to-noise ratio, and furthermore, DWI is overly sensitive to blurring and artifacts, which can affect diagnostic accuracy (44,45).

In conclusion, the present study suggests that the combination of US and MRI can diagnose malignant parotid tumors more accurately compared with either US or MRI alone. These findings suggest that this method can be used to assist in the differential diagnosis of PGTs, thereby facilitating timely and adequate treatment.

**Acknowledgements**

Not applicable.

**Funding**

No funding was received.

**Availability of data and materials**

The data generated in the present study may be requested from the corresponding author.

**Authors' contributions**

JK and QR confirm the authenticity of all the raw data. JK was involved in data curation, formal analysis and writing the original draft. QR contributed to data curation through data cleaning, preprocessing and database management, to methodology through developing the statistical analysis plan, and helped to review and edit the manuscript. ZGC conceptualized the present study. All authors read and approved the final version of this manuscript.

**Ethics approval and consent to participate**

The present study was approved by the ethics committee of Wuhan Central Hospital (approval no. WHZXKYL2023-117). The data are anonymous and the requirement for informed consent was therefore waived.

**Patient consent for publication**

Not applicable.

**Competing interests**

The authors declare that they have no competing interests.

**References**

1. Bradley PJ and McGurk M: Incidence of salivary gland neoplasms in a defined UK population. Br J Oral Maxillofac Surg 51: 399-403, 2013.
2. Inaka Y, Kawata R, Haginomori SI, Terada T, Higashino M, Omura S and Kikuoka Y: Symptoms and signs of parotid tumors and their value for diagnosis and prognosis: A 20-year review at a single institution. Int J Clin Oncol 26: 1170-1178, 2021.
3. Bonavolontà P, Dell'Aversana Orabona G, Maglitto F, Abbate V, Committeri U, Salzano G, Improta G, Iaconetta G and Califano L: Postoperative complications after removal of pleomorphic adenoma from the parotid gland: A long-term follow up of 297 patients from 2002 to 2016 and a review of publications. Br J Oral Maxillofac Surg 57: 998-1002, 2019.
4. Luers JC, Guntinas-Lichius O, Klussmann JP, Küsgen C, Beutner D and Grosheva M: The incidence of Warthin tumours and pleomorphic adenomas in the parotid gland over a 25-year period. Clin Otolaryngol 41: 793-797, 2016.
5. Ferreira PC, Amarante JM, Rodrigues JM, Pinho CJ, Cardoso MA and Reis JC: Parotid surgery: Review of 107 tumors (1990-2002). Int Surg 90: 160-166, 2005.
6. Mohammed F, Asaria J, Payne RJ and Freeman JL: Retrospective review of 242 consecutive patients treated surgically for parotid gland tumours. J Otolaryngol Head Neck Surg 37: 340-346, 2008.
7. Maahs GS, Oppermann Pde O, Maahs LG, Machado Filho G and Ronchi AD: Parotid gland tumors: A retrospective study of 154 patients. Braz J Otorhinolaryngol 81: 301-306, 2015.
8. Choi SY, Lee E, Kim E, Chung MK, Son YI, Baek CH and Jeong HS: Clinical outcomes of bulky parotid gland cancers: Need for self-examination and screening program for early diagnosis of parotid tumors. BMC Cancer 21: 178, 2021.
9. Witt RL: Facial nerve function after partial superficial parotidectomy: An 11-year review (1987-1997). Otolaryngol Head Neck Surg 121: 210-213, 1999.
10. David E, Cantisani V, De Vincentiis M, Sidhu PS, Greco A, Tombolini M, Drudi FM, Messineo D, Gigli S, Rubini A, *et al*: Contrast-enhanced ultrasound in the evaluation of parotid gland lesions: An update of the literature. Ultrasound 24: 104-110, 2016.
11. Stoia S, Lenghel M, Dinu C, Tamaș T, Bran S, Băciuț M, Boțan E, Leucuța D, Armencea G, Onișor F and Băciuț G: The value of multiparametric magnetic resonance imaging in the preoperative differential diagnosis of parotid gland tumors. Cancers (Basel) 15: 1325, 2023.
12. Lee YY, Wong KT, King AD and Ahuja AT: Imaging of salivary gland tumours. Eur J Radiol 66: 419-436, 2008.
13. Quer M, Vander Poorten V, Takes RP, Silver CE, Boedeker CC, de Bree R, Rinaldo A, Sanabria A, Shaha AR, Pujol A, *et al*: Surgical options in benign parotid tumors: A proposal for classification. Eur Arch Otorhinolaryngol 274: 3825-3836, 2017.
14. McGurk M, Thomas BL and Renehan AG: Extracapsular dissection for clinically benign parotid lumps: Reduced morbidity without oncological compromise. Br J Cancer 89: 1610-1613, 2003.
15. Vander Poorten V, Jankowska P and Metcalf R: Salivary gland. In: Stell and Maran's head and neck surgery and oncology. 6th edition. CRC Press, Boca Raton, FL, 2025.
16. Witt RL: Minimally invasive surgery for parotid pleomorphic adenoma. Ear Nose Throat J 84: 308, 310-311, 2005.
17. Di Santo D, Deretti A and Vander Poorten V: Current surgical management of malignant parotid tumors. Curr Opin Otolaryngol Head Neck Surg 33: 79-84, 2025.
18. Roh JL, Kim HS and Park CI: Randomized clinical trial comparing partial parotidectomy versus superficial or total parotidectomy. Br J Surg 94: 1081-1087, 2007.

19. Lombardi D, McGurk M, Vander Poorten V, Guzzo M, Accorona R, Rampinelli V and Nicolai P: Surgical treatment of salivary malignant tumors. Oral Oncol 65: 102-113, 2017.
20. Huyett P, Duvvuri U, Ferris RL, Johnson JT, Schaitkin BM and Kim S: Perineural invasion in parotid gland malignancies. Otolaryngol Head Neck Surg 158: 1035-1041, 2018.
21. Park W, Park J, Park SI, Kim H, Bae H, Cho J, Won H, Park M and Jeong HS: Clinical outcomes and management of facial nerve in patients with parotid gland cancer and pretreatment facial weakness. Oral Oncol 89: 144-149, 2019.
22. Freling NJ, Molenaar WM, Vermey A, Mooyaart EL, Panders AK, Annyas AA and Thijn CJ: Malignant parotid tumors: Clinical use of MR imaging and histologic correlation. Radiology 185: 691-696, 1992.
23. Okahara M, Kiyosue H, Hori Y, Matsumoto A, Mori H and Yokoyama S: Parotid tumors: MR imaging with pathological correlation. Eur Radiol 13 (Suppl 4): L25-L33, 2003.
24. Gritzmann N, Rettenbacher T, Hollerweger A, Macheiner P and Hübner E: Sonography of the salivary glands. Eur Radiol 13: 964-975, 2003.
25. Andreasen S, Therkildsen MH, Bjørndal K and Homøe P: Pleomorphic adenoma of the parotid gland 1985-2010: A Danish nationwide study of incidence, recurrence rate, and malignant transformation. Head Neck 38 (Suppl 1): E1364-E1369, 2016.
26. Moeller K, Esser D, Boeger D, Buentzel J, Hoffmann K, Jecker P, Mueller A, Radtke G, Piesold JU, Schultze-Mosgau S, *et al*: Parotidectomy and submandibulectomy for benign diseases in Thuringia, Germany: A population-based study on epidemiology and outcome. Eur Arch Otorhinolaryngol 270: 1149-1155, 2013.
27. Barnes L, Eveson JW, Reichart PA and Sidransky D (eds): Pathology and Genetics of Head and Neck Tumours. In: WHO Classification of Tumours. 3rd edition, Vol 9. IARC, Lyon, 2005.
28. Takahama Junior A, Almeida OP and Kowalski LP: Parotid neoplasms: Analysis of 600 patients attended at a single institution. Braz J Otorhinolaryngol 75: 497-501, 2009.
29. Committeri U, Arena A, Iaquino V, Salzano G, Blasi FD, Esposito M, Giovacchini F, Calvanese C, Abbate V, Bonavolontà P, *et al*: Surgical management and side effects of parotid gland surgery for benign lesions: A retrospective analysis of our experience from 2012 to 2021. Br J Oral Maxillofac Surg 61: 411-415, 2023.
30. Lee DH, Jung EK, Lee JK and Lim SC: Comparative analysis of benign and malignant parotid gland tumors: A retrospective study of 992 patients. Am J Otolaryngol 44: 103690, 2023.
31. Valstar MH, de Ridder M, van den Broek EC, Stuiver MM, van Dijk BAC, van Velthuysen MLF, Balm AJM and Smeele LE: Salivary gland pleomorphic adenoma in the Netherlands: A nationwide observational study of primary tumor incidence, malignant transformation, recurrence, and risk factors for recurrence. Oral Oncol 66: 93-99, 2017.
32. Gunn A and Parrott NR: Parotid tumours: A review of parotid tumour surgery in the Northern regional health authority of the United Kingdom 1978-1982. Br J Surg 75: 1144-1146, 1988.
33. Cantisani V, David E, Sidhu PS, Sacconi B, Greco A, Pandolfi F, Tombolini M, Lo Mele L, Calliada F, Brunese L, *et al*: Parotid gland lesions: Multiparametric ultrasound and MRI features. Ultraschall Med 37: 454-471, 2016.
34. Rzepakowska A, Osuch-Wójcikiewicz E, Sobol M, Cruz R, Sielska-Badurek E and Niemczyk K: The differential diagnosis of parotid gland tumors with high-resolution ultrasound in otolaryngological practice. Eur Arch Otorhinolaryngol 274: 3231-3240, 2017.
35. Zajkowski P, Jakubowski W, Białek EJ, Wysocki M, Osmólski A and Serafin-Król M: Pleomorphic adenoma and adenolymphoma in ultrasonography. Eur J Ultrasound 12: 23-29, 2000.
36. Brennan PA, Ammar M and Matharu J: Contemporary management of benign parotid tumours - the increasing evidence for extracapsular dissection. Oral Dis 23: 18-21, 2017.
37. Cortcu S, Elmali M, Tanrivermis Sayit A and Terzi Y: The role of real-time sonoelastography in the differentiation of benign from malignant parotid gland tumors. Ultrasound Q 34: 52-57, 2018.
38. Rong X, Zhu Q, Ji H, Li J and Huang H: Differentiation of pleomorphic adenoma and Warthin's tumor of the parotid gland: Ultrasonographic features. Acta Radiol 55: 1203-1209, 2014.
39. Fayad LM, Carrino JA and Fishman EK: Musculoskeletal infection: Role of CT in the emergency department. Radiographics 27: 1723-1736, 2007.
40. Xu Z, Jin Y, Wu W, Wu J, Luo B, Zeng C, Guo X, Gao M, Guo S and Pan A: Machine learning-based multiparametric traditional multislice computed tomography radiomics for improving the discrimination of parotid neoplasms. Mol Clin Oncol 15: 245, 2021.
41. Muntean DD, Dudea SM, Băciuț M, Dinu C, Stoia S, Solomon C, Csaba C, Rusu GM and Lenghel LM: The role of an MRI-based radiomic signature in predicting malignancy of parotid gland tumors. Cancers (Basel) 15: 3319, 2023.
42. Zhang R, Ai QYH, Wong LM, Green C, Qamar S, So TY, Vlantis AC and King AD: Radiomics for discriminating benign and malignant salivary gland tumors; which radiomic feature categories and MRI sequences should be used? Cancers (Basel) 14: 5804, 2022.
43. Karaman CZ, Tanyeri A, Özgür R and Öztürk VS: Parotid gland tumors: Comparison of conventional and diffusion-weighted MRI findings with histopathological results. Dentomaxillofac Radiol 50: 20200391, 2021.
44. Koh DM and Collins DJ: Diffusion-weighted MRI in the body: Applications and challenges in oncology. AJR Am J Roentgenol 188: 1622-1635, 2007.
45. Baliyan V, Das CJ, Sharma S and Gupta AK: Diffusion-weighted imaging in urinary tract lesions. Clin Radiol 69: 773-782, 2014.